

Global-scale shifts in Anthropocene rooting depths pose unexamined consequences in critical zone functioning

Emma Hauser¹, Pamela L Sullivan², Alejandro N. Flores³, and Sharon A Billings¹

¹University of Kansas

²Oregon State University

³Boise State University

November 24, 2022

Abstract

Rooting depth is an ecosystem trait that determines the extent of soil development and carbon cycling. Recent hypotheses propose that human-induced changes to Earth's biogeochemical cycles propagate deeply due to rooting depth changes from agricultural and climate-induced land cover changes. Yet, the lack of a global-scale quantification of rooting depth responses to human activity limits knowledge of hydrosphere-atmosphere-lithosphere feedbacks in the Anthropocene. Here we use land cover datasets to demonstrate that global rooting depths have become shallower in the Anthropocene, and are likely to become yet shallower this century. Specifically, globally averaged depths above which 99% of root biomass occurs (D99) are 8.7%, or 16 cm, shallower relative to those for potential vegetation. This net shallowing results from agricultural expansion truncating D99 by 82 cm, and woody encroachment linked to anthropogenic climate change extending D99 by 65 cm. Projected land cover scenarios in 2100 suggest further D99 shallowing of 63 to 72 cm, exceeding that experienced to date and suggesting that the pace of root shallowing will quicken in the coming century. Losses of Earth's deepest roots—soil-forming agents—suggest unanticipated changes in fluxes of water, solutes, and carbon. Our work constrains rooting depth distributions for global models, allowing the land modeling community to explore cascading effects of rooting depth changes on water, carbon, and energy dynamics, and can guide design of field-based efforts to quantify deep anthropogenic influences. Understanding human influence on biota's reach into Earth's subsurface will improve predictions of interactive functioning of the biosphere, lithosphere, and hydrosphere.

1 **Global-scale shifts in Anthropocene rooting depths pose unexamined consequences in**
2 **critical zone functioning**

3 Emma Hauser^{1,2}, Pamela L. Sullivan³, Alejandro Flores⁴, Sharon A. Billings^{1,2}

4 ¹The University of Kansas, Department of Ecology and Evolutionary Biology, Lawrence, KS,
5 USA.

6 ²The Kansas Biological Survey, Lawrence, KS, USA.

7 ³College of Earth, Ocean, and Atmospheric Science, Oregon State University, Corvallis, OR,
8 USA.

9 ⁴Department of Geosciences, Boise State University, Boise, ID, USA

10 Corresponding author: Sharon A. Billings, Emma Hauser (sharon.billings@ku.edu,
11 emhauser@ku.edu)

12 **Key Points:**

- 13 • Globally averaged rooting depths have become shallower by 16 cm in the Anthropocene
14 and will be truncated by up to 72 cm by 2100.
- 15 • In agricultural lands, the depth to which 99% of crop roots extend is shallower by up to
16 82 cm compared to natural systems.
- 17 • Where woody encroachment is occurring, analogous rooting zones are deepened by up to
18 65 cm compared to previous dominant vegetation.
- 19

20 Abstract

21 Rooting depth is an ecosystem trait that determines the extent of soil development and carbon
22 cycling. Recent hypotheses propose that human-induced changes to Earth's biogeochemical
23 cycles propagate deeply due to rooting depth changes from agricultural and climate-induced land
24 cover changes. Yet, the lack of a global-scale quantification of rooting depth responses to human
25 activity limits knowledge of hydrosphere-atmosphere-lithosphere feedbacks in the
26 Anthropocene. Here we use land cover datasets to demonstrate that global rooting depths have
27 become shallower in the Anthropocene, and are likely to become yet shallower this century.
28 Specifically, globally averaged depths above which 99% of root biomass occurs (D99) are 8.7%,
29 or 16 cm, shallower relative to those for potential vegetation. This net shallowing results from
30 agricultural expansion truncating D99 by 82 cm, and woody encroachment linked to
31 anthropogenic climate change extending D99 by 65 cm. Projected land cover scenarios in 2100
32 suggest further D99 shallowing of 63 to 72 cm, exceeding that experienced to date and
33 suggesting that the pace of root shallowing will quicken in the coming century. Losses of
34 Earth's deepest roots—soil-forming agents—suggest unanticipated changes in fluxes of water,
35 solutes, and carbon. Our work constrains rooting depth distributions for global models, allowing
36 the land modeling community to explore cascading effects of rooting depth changes on water,
37 carbon, and energy dynamics, and can guide design of field-based efforts to quantify deep
38 anthropogenic influences. Understanding human influence on biota's reach into Earth's
39 subsurface will improve predictions of interactive functioning of the biosphere, lithosphere, and
40 hydrosphere.

41 Plain Language Summary

42 The depth of plant roots helps determine the extent of nutrient, carbon and water cycling beneath
43 Earth's surface. Human activities, including land use and climate change, can change the
44 distribution of plant roots and their activities across the globe. Here, we used global land cover
45 datasets in combination with field-generated rooting depth equations to estimate global scale
46 changes to roots both now and into the future. Globally, roots are shallower than they would be
47 in the absence of human activity due to extensive land conversion to agriculture. In some
48 regions, human-promoted woody encroachment induces root elongation, but this effect is
49 overwhelmed by the spatial extent of agricultural conversion. In the future, roots will become

50 shallower at an even faster pace. In both contemporary and future projections, deep roots are
51 especially vulnerable to loss, suggesting that the extent of element and water cycles may get
52 shallower in the future, too. This opens numerous questions for additional field- and modeling-
53 based studies about the ways nutrients, carbon, and water will cycle in a future with fewer deep
54 roots. We provide a foundation for those questions by demonstrating humans' influence on the
55 roots that shape the character of Earth's skin.

56 **1 Introduction**

57 Roots are subsurface engineers, and their depth distributions drive ecosystem-scale processes
58 (Maeght et al., 2013; Pierret et al., 2016) such as soil development (Brantley et al., 2017;
59 Hasenmueller et al., 2017; Austin et al., 2018), release of mineral-bound nutrients (Jobbagy and
60 Jackson, 2001; Hasenmueller et al., 2017; Austin et al. 2018), subsoil water flow paths and
61 residence time (Zhang et al., 2015; Fan et al., 2017) , and deep C fluxes (Richter and Markewitz,
62 1995; Schenk, 2007; Pierret et al., 2016; Fan et al., 2017; Billings et al., 2018). The dominant
63 drivers of rooting depths are plant functional type (PFT, Jackson et al., 1996) and variation in
64 water availability (Schenk, 2007; Nippert et al., 2007; Fan et al., 2017), both of which are
65 changing in response to anthropogenic land cover conversion and altered atmospheric
66 composition (Edgeworth et al, 2001; Cramer et al., 2010; Ellis et al., 2010). This observation
67 suggests that rooting depth distributions should be undergoing changes due to human activities in
68 the critical zone (CZ, Earth's living skin, Jordan et al., 2001).

69
70 In spite of widespread recognition of the importance of root depth (Maeght et al., 2013; Pierret et
71 al., 2016) and a growing recognition of the great depths to which roots can penetrate (Nepstad et
72 al., 1994; Canadell et al., 1996), large-scale responses of rooting depths to anthropogenic
73 perturbations of the biosphere have been poorly characterized. This knowledge gap is due in part
74 to the challenges of accessing relatively deep soil horizons (Maeght et al., 2013), as well as the
75 challenge of unraveling the vast complexity of Earth's subsurface systems. One consequence of
76 poorly defined rooting depths at large spatial scales is generalized representations of rooting
77 parameters in Earth Systems Models (ESMs; Smithwick et al., 2014; Clark et al., 2015). Given
78 the plethora of CZ functions influenced by roots (Maeght et al., 2013; Pierret et al., 2016), poor
79 characterization of rooting depths likely limits the accuracy of projected responses of the coupled
80 terrestrial water, energy, and carbon cycles to climate in the Anthropocene.

81

82 Quantifying large-scale, human-induced changes to rooting depths and how they may differ
83 regionally is a critical step towards a greater understanding of how roots govern large-scale, sub-
84 surface and surface processes. For example, a recent hypothesis proposes that anthropogenic
85 changes to land cover that modify rooting depth distributions can alter natural elemental cycles
86 deep belowground in ways important for soil and ecosystem development (Billings et al., 2018).
87 Testing this hypothesis on a regional or global scale requires global-scale estimates of changes in
88 rooting depths due to human activities. If explicitly calculated, these estimates would be a key
89 component of projecting material fluxes via land surface models, and for elucidating the most
90 critical foci for future laboratory and field efforts necessary to enhance our understanding of
91 global change agents.

92

93 Two Anthropocene phenomena occur at sufficient magnitude to alter rooting depths in ways
94 complicating their quantification. First, many regions have experienced conversion to annual row
95 crops (Ramankutty and Foley, 1999; Ellis et al., 2010), a process that induces mortality of deep
96 perennial root systems and replaces them with relatively shallow roots (Billings et al., 2018). In
97 contrast, climate change and increasing atmospheric CO₂ concentrations are linked to root
98 extension of extant woody plants (Iversen, 2010), and shifting ecoregion ranges may increase
99 rooting depths where more deeply rooted woody vegetation becomes increasingly abundant in
100 grasslands and tundra (Jackson et al., 1996; Harsch et al., 2009; Stevens et al., 2017; Wang et al.,
101 2019). Studies exploring rooting depth typically focus on absolute rooting depths and their
102 responses to climate or atmospheric CO₂ (Kleidon and Heimann, 1998; Kleidon, 2003) or,
103 separately, land cover changes in specific regions of interest (Jeremillo et al., 2003; Hertel et al.,
104 2009; DuPont et al., 2010). Despite known changes in global land cover (Ellis et al., 2010) that
105 are associated with distinct rooting depths (Jackson et al., 1996), to date, no one has directly
106 quantified the net change in contemporary root depth distributions at the global scale as a
107 consequence of these opposing human activities.

108

109 Here, we estimate the extent to which rooting depths increase or decrease in response to land use
110 and climate change. We also project how rooting depths may change throughout the 21st century
111 as more land is converted to agricultural and urban use, and as biome ranges continue to shift

112 with changing climate. We emphasize that our focus is not on maximum rooting depths. Indeed,
113 there is a growing appreciation of the great depths to which vegetation can root (Maeght et al.,
114 2013; Pierret et al., 2016; Fan et al., 2017), though the true maximum rooting depth may never
115 be known in some systems (Kleidon, 2003; Pierret et al., 2016; Fan et al., 2017). Instead, we
116 focus on the depths to which most or half (i.e., 99%, 95%, and 50%) of ecosystems' root biomass
117 extends, metrics that highlight very deep roots as well as the depths at which most roots reside,
118 both of which are functionally consequential measures. These metrics represent those for which
119 much data exist, and facilitate the cross-system comparisons necessary to estimate the extent of
120 rooting depth changes in the Anthropocene. Our work thus reveals how anthropogenic, global-
121 scale changes in rooting depth metrics have influenced, and will continue to influence, spatially
122 varying patterns of the belowground activities of ecosystems, thereby illuminating critical next
123 steps to help us understand future CZ functioning.

124 **2 Materials and Methods**

125 We estimated potential (i.e., no human influence), contemporary, and projected root distributions
126 at the global scale by combining biome-specific rooting depth functions derived from empirical
127 studies (described below) with spatially explicit land cover datasets. We used satellite-derived,
128 potential vegetation representing 15 land cover classes (Haxeltine and Prentice, 1996) and their
129 potential global distribution in the absence of human activity at a 5-minute spatial resolution
130 (Ramankutty and Foley, 1999). We compared potential vegetation classes to contemporary land
131 cover as defined by the Global Land Cover 2000 (GLC2000) dataset (Bartolome and Belward,
132 2005). GLC2000 represents 22 land cover types, which are designated according to plant
133 functional types ascribed to satellite images and ground-truthed by regional analysts. We aligned
134 contemporary vegetation classifications with potential vegetation classes according to previously
135 published frameworks for ecoregion designation (Bartolome and Belward, 2005), and augmented
136 these classes to include a class for permafrost regions where rooting depth may be limited. These
137 efforts resulted in 25 distinct land cover types for which rooting depths were assigned. Projected
138 vegetation classes were similarly developed for four Shared Socioeconomic Pathway (SSP) and
139 Representative Concentrations Pathway (RCP) scenarios using spatial projections of gridded,
140 0.5° x 0.5° resolution land covers for the year 2100 (Hurtt et al., 2011).

141

142 For all vegetation datasets except those above 60°N latitude (described below), we estimated
143 biome-specific rooting depths by assigning rooting depth functions derived from empirical data
144 (Zheng, 2001). Specifically, we estimated the depths by which rooting systems exhibit 50%
145 (D50), 95% (D95) and 99% (D99) of their total biomass in each land cover type. Invoking these
146 functions (Zheng 2001) assumes that rooting depth distributions remain similar for each
147 vegetation functional type in the potential, contemporary, and future scenarios. The merit of this
148 assumption may vary with time, but keeping each biome's rooting depth consistent across the
149 Holocene and into the future allows us to parse the influence of land cover change on rooting
150 depths from that of less well-characterized phenomena.

151
152 We modified the estimated rooting depth distributions for four of the 25 land covers. First, the
153 land cover datasets combine both polar and mid-latitude deserts into a single desert category
154 based on hydrologic regimes, yet rooting depths in polar deserts are often constrained by
155 permafrost. We thus separated these two desert regions, reassigning deserts in polar regions to
156 the 'tundra' classification above 60 degrees north, a point above which frozen soils often limit
157 deep root development (Zhang et al., 2008). Second, because many remote sensing-based studies
158 omit large, lower latitude desert regions from their analyses due to the lack of quantifiable
159 ecosystem productivity in these systems (Zhao et al., 2005), we omitted true deserts from rooting
160 depth averages reported in the main text. Instead, we present rooting depth metrics that
161 incorporate mid-latitude deserts' potential contribution to global root averages in Table 1 of the
162 Supporting Information. Comparison of these results with those reported in the text reveal an
163 inflated influence of mid-latitude desert rooting depth estimates on global averages that likely
164 does not represent reality due to the low density of plants in true deserts (Whitford and Duval,
165 2019). Finally, we reassigned evergreen forest and mixed vegetation classes above 50°N to the
166 'boreal' vegetation classification, and ecoregions above 60°N to the class 'tundra.' We gave all
167 classes above 60°N a rooting depth specific to permafrost-underlain regions, where roots
168 typically do not penetrate deeper than 30 cm (Billings et al., 1997; Boike et al., 2018).

169
170 To assess potential effects of global-scale perturbations projected by the year 2100 on rooting
171 depth distributions, we examined multiple SSP and RCP land cover projections from the
172 Intergovernmental Panel on Climate Change (IPCC). Projected vegetation classes were

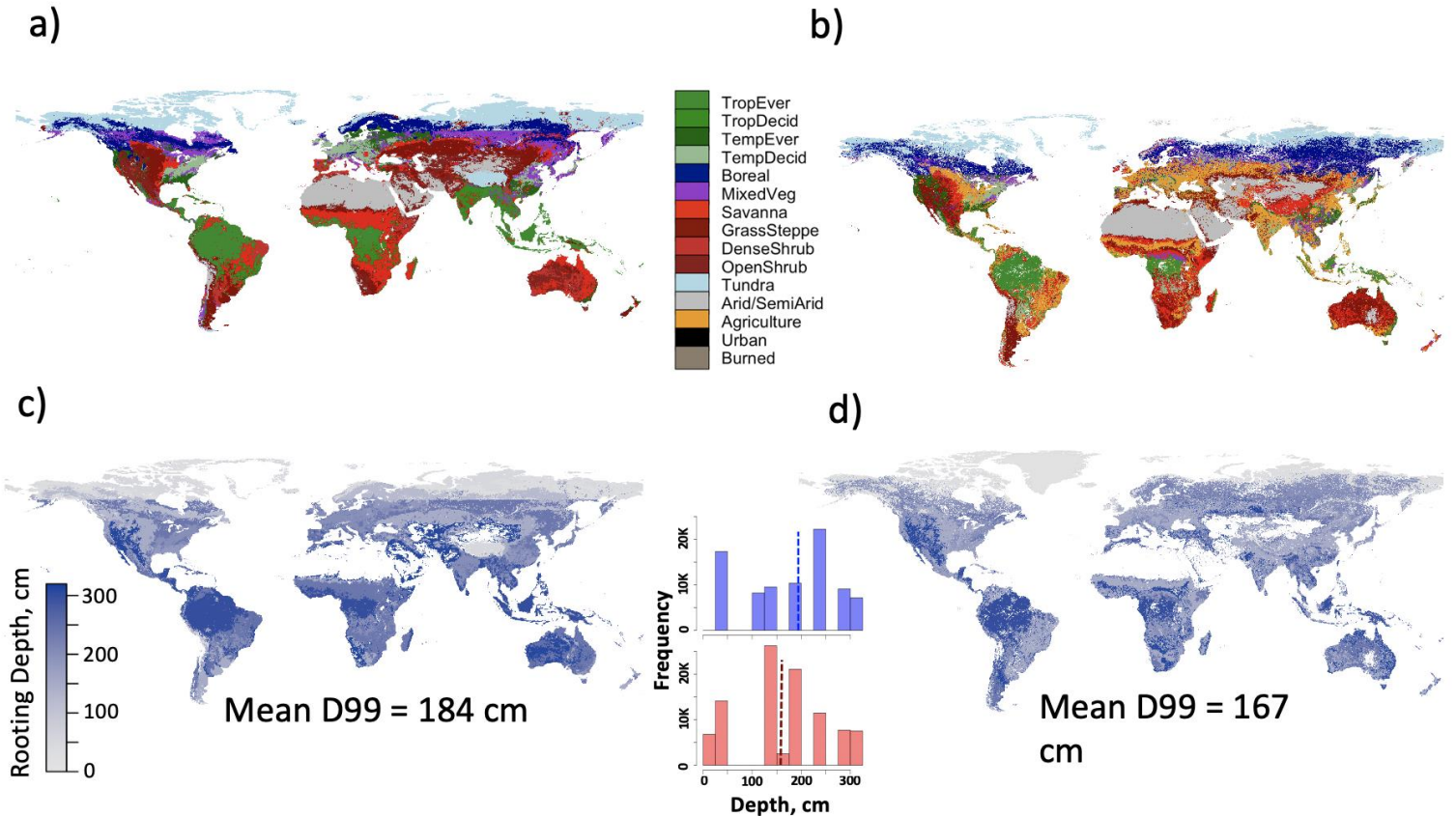
173 developed for 4 SSP RCP scenarios (SSP2 RCP4.5, SSP1 RCP2.6, SSP4 RCP6.0, SSP5
174 RCP8.5). Landuse harmonization datasets designate land cover classes more coarsely than either
175 GLC2000 or potential vegetation datasets, delineating primary and secondary forest regions,
176 primary and secondary non-forest regions, 5 agricultural classes, pasture land, rangeland, and
177 urban regions (Hurtt et al., 2011). We assigned a rooting depth equation derived from
178 agricultural croplands (Zheng, 2001) to all 5 agricultural classes in the landuse harmonization
179 dataset. For secondary non-forests, we assigned rooting depth equations representing herbaceous
180 and grassland systems, and pastures and rangeland were assigned rooting depth equations
181 derived from C4 grasslands and pastures (Zheng, 2001). Because most secondary forests in these
182 scenarios were in the boreal region, we assigned the average root depth value of mixed forests
183 (240 cm) and boreal forests (119 cm) to secondary forests. Reflecting anticipated warming, root
184 depths assigned in all future scenarios removed permafrost constraints (Lawrence and Slater,
185 2005).

186
187 Using R's raster package (RStudio Team, 2017; Hijmans et al., 2019) we assigned rooting depth
188 values to each land cover classification of the potential, contemporary, and projected vegetation
189 maps, and calculated global means of each depth metric. We then compared metrics across time
190 using 95% confidence intervals of the mean estimates of global rooting depth metrics. We
191 performed correlated t-tests on pairs of rasters (i.e. potential vs. contemporary, and contemporary
192 vs. projected) to determine whether differences between these estimated rooting depth metrics
193 are significantly different from zero. Data were assessed to ensure they met the assumptions of
194 correlated t-tests.

195 **3 Results**

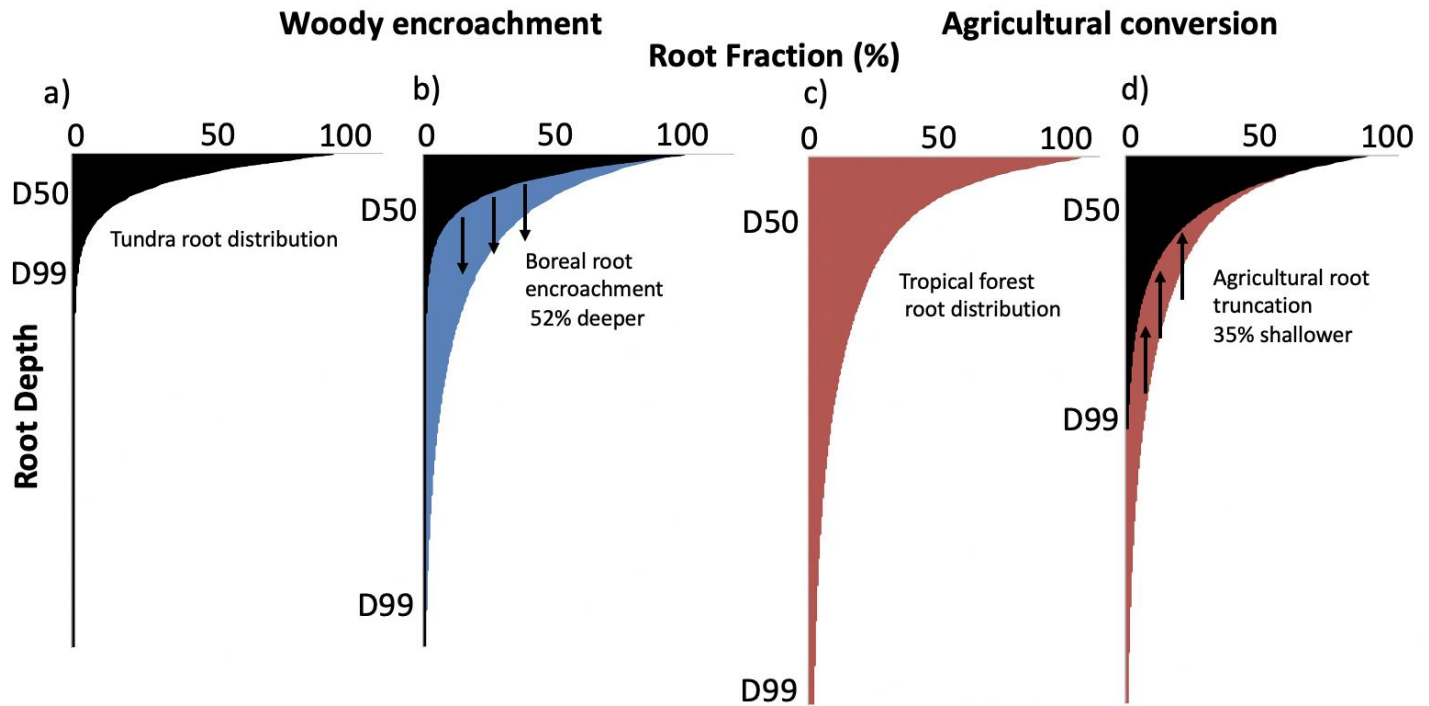
196 Comparisons of potential and contemporary land cover (Figures 1a and b) and their estimated
197 rooting depths (Figures 1c and d) suggest that spatially averaged, global values of D99 are up to
198 8.7% shallower (16 cm) under contemporary land cover distributions than if potential vegetation
199 cover types covered Earth's terrestrial surface ($t = -128.08$, $P < 0.0001$; Figures 1c and d, Table
200 S1). Values of D95 for contemporary land cover also express trends of root shallowing, though
201 less so than D99 (7.8% or 8 cm; $t = -85.342$, $P < 0.0001$; Figures S1a and b). Depth to 50% root
202 biomass (D50), by comparison, displays relatively little variation between contemporary and

203 potential land cover, becoming less than 1 cm shallower (2.5%; $t = -111.75$, $P < 0.0001$) on
 204 average (Figure S2). The comparatively small change in globally averaged D50 values is a
 205 consequence of relatively rapid root establishment in shallow horizons of cultivated systems.



206
 207 **Figure 1.** Land cover and associated rooting depths under potential vegetation in the absence of human influence
 208 (left column) and today's vegetation distribution (right column). (a) Potential vegetation cover in the absence of
 209 human activity modified to accommodate permafrost regions, where all plants regardless of functional type are
 210 depth-limited by frozen soils. (b) Contemporary land cover distribution from Global Land Cover 2000 (GLC2000),
 211 modified to correspond to potential vegetation land cover classifications. Subsequent maps depict depths by which
 212 99% of rooting biomass occurs (D99) under potential (c) and contemporary (d) land cover types. Inset histogram
 213 displays rooting depth distributions. Blue histograms reflect potential vegetation data, and red histograms
 214 contemporary land cover. Dashed lines represent means. Appearance of a distinct line at 50°N in potential
 215 vegetation rooting depth coverages is an artifact of restricted maximum rooting depth assignments to reflect
 216 limitations imposed by frozen soils. Note that most of Greenland is assigned a rooting depth of zero in all maps
 217 because of ice cover, which is denoted in white and grey in potential and contemporary root coverages, respectively.
 218

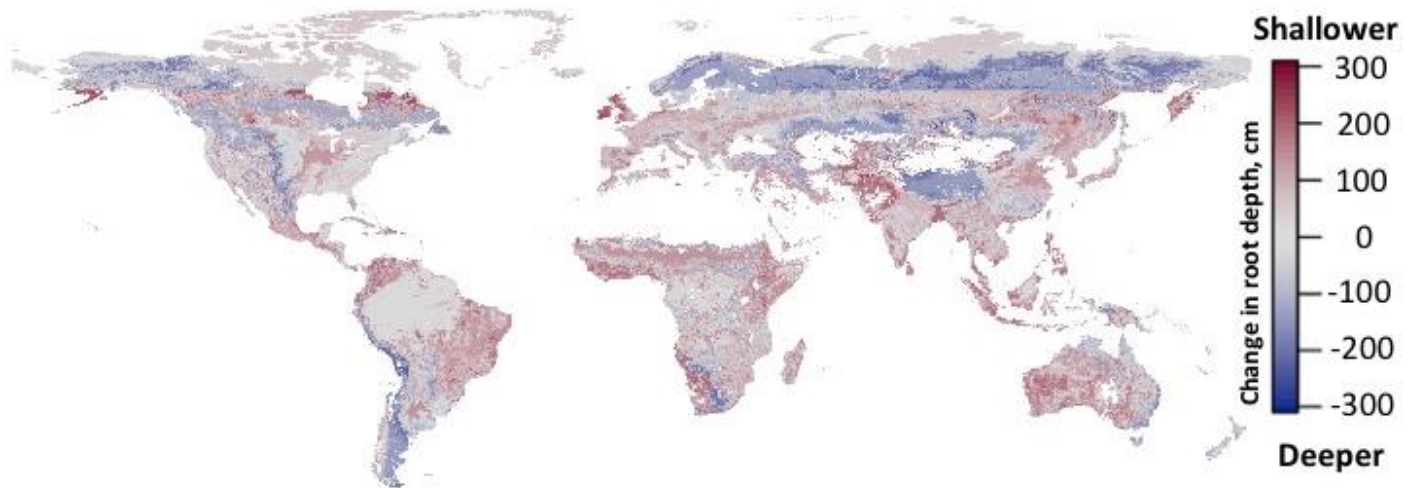
219 Agricultural land conversion serves as the dominant influence on these global trends (Figures 2
 220 and 3). Where perennial vegetation has been converted to agricultural land (defined here as
 221 annual crops and managed pasture), D99 has decreased by as much as 35% (82 cm) across $2.4 \times$
 222 10^9 ha (15% of Earth's terrestrial surface). In contrast, where woody encroachment is evident in
 223 contemporary land cover data, D99 increased relative to potential vegetation by up to 52% (65
 224 cm). This result is likely an overestimate of current root depths because we assigned rooting
 225 depths derived from well-established systems (Zheng, 2001) although woody plants in recently
 226 encroached systems likely have not yet achieved such depths (Stevens et al., 2017; Billings et al.,
 227 2018). In spite of this possible overestimation, root deepening via woody encroachment does not
 228 overcome the effect of root shallowing in agricultural lands because of the smaller fraction of
 229 Earth's terrestrial surface experiencing woody encroachment (9.3×10^7 ha, or 0.6%).



230

231 **Figure 2.** Representation of rooting depth elongation due to woody encroachment (a and b) and rooting depth
 232 truncation due to agricultural expansion (c and d). Blue region in B demonstrates the belowground increase in roots
 233 shown in blue in Figure 3. Red region in D exemplifies loss of rooting system depth for red regions in Figure 3.

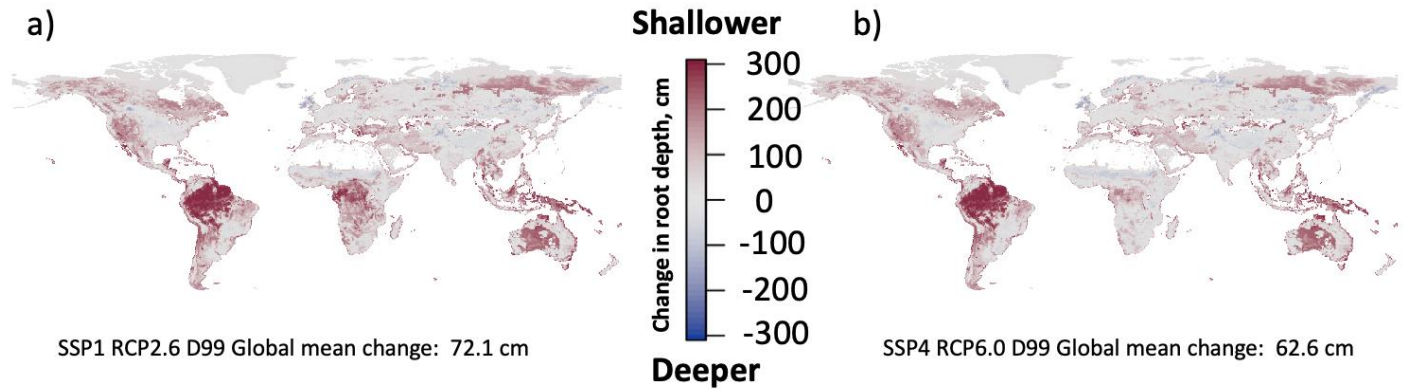
234



235
 236 **Figure 3.** Mapped differences between potential and contemporary rooting depths. Red cells indicate a decrease in
 237 the depth to 99% of rooting biomass (D99) while blue cells indicate an increase in D99 resulting from contemporary
 238 vegetation distributions.

239
 240 Projections for the year 2100 suggest that the scenario with the largest cropland increase and
 241 relatively low radiative forcing enhancement from current levels (SPP1 RCP2.6, Figure 4a)
 242 generates the most extreme shallowing of deep roots, truncating values of D99 by 72 cm (t
 243 = 419.91, $P < 0.0001$). The smallest decline in D99, a shallowing of 63 cm ($t = 370.35$, $P <$
 244 0.0001), occurs under a scenario of moderate cropland increase and stabilization of moderate to
 245 high radiative forcing at 6 Wm^{-2} by 2100 (SPP4 RCP6.0, Figure 4b). The highest emissions
 246 scenario (SSP5 RCP8.5) produces an intermediate D99 shallowing of 64 cm, the result of
 247 extensive conversion of forests into cropland (Figure S4) and root elongation in boreal and high-
 248 elevation regions (compare Figure 3 and Figure S4). Widespread, substantial root shallowing is
 249 evident in many regions but is particularly evident across the Amazon basin, consistent with
 250 multiple projections of rapidly transitioning vegetation cover in that region (Hurtt et al., 2011).

251



252
253

254

255 **Figure 4.** Projected changes of depth to 99% rooting biomass (D99) by the year 2100 relative to contemporary
 256 rooting depth distributions. Projections are based on land use and emissions changes under two combinations of
 257 Shared Socioeconomic Pathways (SSP) and Representative Concentration Pathways (RCP), SSP1 RCP2.6 (a) and
 258 SSP4 RCP6.0 (b). These two maps represent the scenario of greatest projected change and least projected change.
 259 Grey and red colors indicate root depth truncation and blue indicates elongation.

260

261 Values of D50 for the year 2100 also reflect a consistent response to the rapidly transitioning
 262 vegetation that likely drives projected changes in D99 and D95, leading to a D50 shallowing of 5
 263 to 6 cm across all assessed scenarios ($t = 416.2$, $P < 0.0001$; Figure S5). Though small relative to
 264 changes in deep root systems, this D50 shallowing is 4 to 5 cm more severe than that occurring
 265 during the previous $\sim 10,000$ y (Gupta, 2004) of anthropogenic land conversion to agriculture
 266 (Figure S6).

267 **4 Discussion**

268 Our rooting depth estimates suggest that the portion of rooting biomass most vulnerable to
 269 human influence is, counterintuitively, deep in the soil profile (Figures 2 and 3). Although
 270 maximum rooting depths are poorly characterized and are likely deeper than is typically
 271 appreciated (Maeght et al., 2013; Pierret et al., 2016; Fan et al., 2017), we demonstrate that
 272 metrics of most or half of all rooting biomass (i.e., D99, D95, and D50), no matter their absolute
 273 value, are currently a reflection of human-induced, global-scale changes in land cover (Figure 1).
 274 We further demonstrate that the globally-averaged estimate of a 16% shallowing of D99 values

275 is the net result of root shallowing in agricultural regions and root elongation in regions of
276 woody encroachment, with the area represented by agriculture dominating the effect.

277
278 With atmospheric CO₂ anticipated to continue increasing in the coming decades, we might
279 expect woody encroachment's elongating effects on D99, D95, and D50 to effectively mitigate
280 the root shallowing effect of land conversion to agriculture. However, the four IPCC scenarios
281 explored here suggest that by 2100, rooting distributions may become yet shallower relative to
282 contemporary rooting depths (Figures 3, S4 and S5). As observed for comparisons between
283 potential and contemporary land cover, the deeper rooting metrics (D99 and D95) display greater
284 changes in their global mean than D50 when comparing contemporary and projected land cover.
285 Thus, both comparisons suggest that the deepest roots are the most vulnerable to loss via
286 anthropogenic changes.

287
288 Unlike contemporary vs. potential vegetation comparisons, D50 metrics in future scenarios are
289 considerably shallower than contemporary scenarios. These results highlight that
290 anthropogenically-induced changes in surficial soil horizons' root abundances in the coming
291 decades will likely exceed those of the past several millennia. They also emphasize that even
292 relatively shallow soil horizons (*i.e.*, those expressed by D50), where both natural and
293 agricultural species root, will undergo redistribution in the coming decades.

294
295 There are myriad feasible consequences of altered rooting depths for biogeochemical and
296 hydrological fluxes that prompt hypotheses for future research efforts. For example, roots
297 beneath the zone of maximum rooting density are attributed with developing the soils that mantle
298 Earth's surface, so much so that they are referred to as the planet's biotic weathering front, where
299 life – roots and microbes – promotes the dissolution of bedrock (Richter and Markewitz, 1995;
300 Berner et al., 2003; Brantley et al., 2012; Pawlik, 2013; Dontsova et al., 2020). Results from the
301 current study suggest that these biotic weathering forces in many regions do not reach as deeply
302 into the regolith as they did prior to human influence, prompting the hypothesis that the intensity
303 of biotic modes of soil formation at the bottom of the soil profile have declined in the
304 Anthropocene. Further, if a smaller volume of soil is explored by rooting systems, it is plausible

305 that soil water storage capacity, nutrient replenishment and solute losses from freshly weathered
306 material could decline (Swank, 1986; Nepstad et al., 1994; Berner, 1998).

307

308 Such implications emphasize the importance of future numerical and empirical experiments
309 exploring the climate and biogeochemical feedbacks of deep root losses. Because terrestrial
310 vegetation exerts a fundamental global control on land-atmosphere exchanges of water, energy,
311 carbon, and other elements, improved representation of rooting distributions in global land
312 models such as the Community Land Model (Lawrence et al., 2019) is of critical importance.
313 This is particularly true as more sophisticated aboveground and belowground vegetation and
314 biogeochemical processes are incorporated into these models (e.g., Tang et al., 2013; Fisher et
315 al., 2017; Kennedy et al., 2019). With improved fidelity to biophysical and biogeochemical
316 processes comes the corresponding opportunity to explore the potential consequences of changes
317 in global rooting depths on land-atmosphere exchanges of water, energy, and carbon, and the
318 large-scale ramifications that changes in rooting depths have for climate. Well-designed
319 numerical experiments would be able to elucidate the relative impacts of exogenous (e.g.,
320 agricultural conversion, woody encroachment) versus endogenous (e.g., water and nutrient
321 limitation) changes in rooting depths on terrestrial cycling of water, energy, and carbon.

322

323 Future empirical studies examining the contribution of deep roots to soil structure, C and nutrient
324 fluxes, and water flow paths also offer opportunities to characterize the biogeochemical
325 consequences of shallowed rooting systems. More extensive empirical work can generate more
326 accurate parameters for representing subsurface biogeochemical fluxes in ESMs, where highly
327 non-linear feedbacks between these changes and climatic conditions can be examined.

328 Specifically, leveraging of on-going climate experiments (e.g., Caplan et al., 2019), naturally
329 existing climatic gradients (e.g., Ziegler et al. 2017), and chronosequences (e.g., Billings et al.
330 2018) could reveal quantitative relationships between rooting depth distributions and their
331 impacts on soil formation processes, especially at depth. Given deep root contributions to soil C,
332 nutrient and water fluxes, as well as soil formation (Maeght et al., 2013; Pierret et al., 2016;
333 Rasse et al., 2005), revealing rooting depth feedbacks to Earth's biogeochemistry is critical for
334 understanding the current and future function of Earth's critical zone.

335 **5 Conclusion**

336 Losses of relatively deep roots suggest an overlooked and subtle mechanism by which humans
337 alter soil and ecosystem development. It is well established that humans accelerate losses of
338 surface soil via erosion, which can result in a thinning of Earth's skin of soil (Wilkinson and
339 McElroy, 2007). In contrast, altered rooting depths deep in soil profiles due to anthropogenic
340 land use and climate change suggest a means by which human actions may govern soil thickness
341 near the bottom of soil profiles. These shifts in root distributions support the idea that signals of
342 the Anthropocene penetrate deeply into the subsurface even in naturally occurring elemental
343 cycles (Billings et al., 2018). Indications of widespread human transformation of land cover
344 across millennia (Edgeworth et al., 2015) imply that reductions in deep root abundances have
345 been underway in multiple regions for a similarly lengthy time. Though improving process
346 representation in land models continues apace (Fisher and Koven, 2020), the representation of
347 rooting depth distributions remains largely a static function of only PFT (although see Drewniak,
348 2019 for an important counterexample). We present an opportunity to advance the
349 representation of roots in land models by better constraining how rooting depth distributions vary
350 with global change, as well as by identifying specific ecological processes particularly suited to
351 better quantifying the dynamics of rooting, both past and future (e.g., regions of woody
352 encroachment). Future co-designed modeling, field and lab studies are needed to help clarify the
353 consequences of rooting depth changes for contemporary and future CZ development. These
354 studies will elucidate the ways that surficial anthropogenic activities radiate deep within Earth's
355 subsurface, altering the developmental pace and character of Earth's critical zone.

356 **Acknowledgments**

357 We thank Drs. Jorge Soberón, A. Townsend Peterson, Dan Richter and Paulyn Cartwright for
358 offering helpful insights. We extend appreciation to Dr. Dan Markewitz for sharing his thoughts
359 about root extension into the subsoil. Funding for this work was provided by NSF 1331846, NSF
360 1841614, and NSF 0919443.

361 **Data Availability and Code Availability**

362 The original GLC2000 dataset modified for this analysis can be accessed at
363 <https://forobs.jrc.ec.europa.eu/products/glc2000/products.php>. The unmodified potential

364 vegetation data can be found at https://daac.ornl.gov/cgi-bin/dsviewer.pl?ds_id=961. All future
 365 land use projections can be accessed through the Landuse Harmonization data portal at
 366 <http://luh.umd.edu/data.shtml>. Rasters modified as described in Methods for contemporary and
 367 potential land cover, along with root depth assignment .csv files and code are available on
 368 Zenodo (<https://doi.org/10.5281/zenodo.3975240>).

369 **Author Contributions**

370 SAB and EMH conceived of the idea with input from PLS. Analyses were developed and
 371 implemented by EMH and SAB. The manuscript was written by EMH and SAB with input from
 372 PLS and AF.

373 **References**

- 374 Austin, J.J.C., Perry, A., Richter, D. D. & Schroeder, P. A. (2018). Modifications of 2:1 clay
 375 minerals in a kaolinite-dominated Ultisol under changing landuse regimes. *Clays and*
 376 *Clay Minerals*, 66, 61-73. doi: 10.1346/CCMN.2017.064085
 377
- 378 Bartolome, E. & Belward, A.S. (2005). GLC2000: A new approach to global land cover
 379 mapping from Earth observation data. *International Journal of Remote Sensing* 26, 1959-
 380 1977. doi: 10.1080/01431160412331291297
 381
- 382 Berner, R. A. (1998). The carbon cycle and carbon dioxide over Phanerozoic time: the role of
 383 land plants. *Philosophical Transactions of the Royal Society of London. Series B:*
 384 *Biological Sciences* 353, 75-82.
- 385 Berner, E. K., Berner, R. A., & Moulton, K. L. (2003). Plants and mineral weathering: present
 386 and past. *TrGeo* 5, 605. doi: 10.1098/rstb.1998.0192
- 387 Billings, S.A., Hirmas, D., Sullivan, P. L., Lehmeier, C. A., Bagchi, S., Min, K., Brecheisen, Z.,
 388 Hauser, E., Stair, R., Flournoy, R. & Richter, D.D. (2018). Loss of deep roots limits
 389 agents of soil development that are only partially restored by decades of forest
 390 regeneration. *Elementa Science of the Anthropocene*, 6, 34.
 391 [doi:10.1525/elementa.287](https://doi.org/10.1525/elementa.287)
- 392 Billings, W. D., Peterson, K. M., Shaver, G. R., & Trent, A. W. (1977). Root growth, respiration,
 393 and carbon dioxide evolution in an arctic tundra soil. *Arctic and Alpine Research* 9, 129-
 394 137.
- 395 Boike, J., Juszak, I., Lange, S., Chadburn, S., Burke, E., Paul Overduin, P., ... & Gouttevin, I.
 396 (2018). A 20-year record (1998–2017) of permafrost, active layer and meteorological
 397 conditions at a high Arctic permafrost research site (Bayelva, Spitsbergen). *Earth System*
 398 *Science Data* 10, 355-390. doi: 10.5194/essd-10-355-2018
 399
- 400 Brantley, S. L., Eissenstat, D. M., Marshall, J. A., Godsey, S. E., Balogh-Brunstad, Z., Karwan,

- 401 D. L., Papuga, S. A., Roering, J., Dawson, T. E., Evaristo, J., Chadwick, O.,
402 McDonnell, J. J., & Weathers, K. C. (2017). Reviews and syntheses: On the roles trees
403 play in building and plumbing the Critical Zone. *Biogeosciences*, *14*, 5115-5142.
404 doi: [10.5194/bg-14-5115-2017](https://doi.org/10.5194/bg-14-5115-2017)
405
- 406 Brantley, S. L., Lebedeva, M., & Hausrath, E. M. (2012). A geobiological view of weathering
407 and erosion. *Fundamentals of Geobiology*, 205-227. doi: 10.1002/9781118280874.ch12
408
- 409 Burke, B. C., Heimsath, A. M., & White, A. F. (2007). Coupling chemical weathering with soil
410 production across soil-mantled landscapes. *Earth Surface Processes and Landforms: The*
411 *Journal of the British Geomorphological Research Group* *32*, 853-873. doi:
412 10.1002/esp.1443
413
- 414 Canadell, J., Jackson, R. B., Ehleringer, J. B., Mooney, H. A., Sala, O. E. & Schulze E-D.
415 (1996). Maximum rooting depth of vegetation types at the global scale. *Oecologia*, *108*,
416 583-595. doi: 10.1007/BF00329030
417
- 418 Caplan, J.S., Gimenez, D., Hirmas, D.R., Brunsell, N.A., Blair, J.M. & Knapp, A.K. (2019).
419 Decadal-scale shifts in soil hydraulic properties as induced by altered precipitation. *Sci*
420 *Adv.* *5*:eaau6635. doi:10.1126/sciadv.aau6635.
421
- 422 Clark, M. P., Fan, Y., Lawrence, D. M., Adam, J. C., Bolster, D., Gochis, D. J., et al. (2015).
423 Improving the representation of hydrologic processes in Earth System Models. *Water*
424 *Resources Research* *51*, 5929-5956. doi: 10.1002/2015WR017096
425
- 426 Cramer, W., Bondeau, A., Woodward, I., Prentice, I., Betts, R., Brovkin, V., Cox, P., Fisher, V.,
427 Foley, J., Friend, A., Kucharik, C., Lomas, M., Ramankutty, N., Sitch, S., Smith, B.,
428 White, A. & Young-Molling, C.(2001). Global response of terrestrial ecosystem structure
429 and function to CO₂ and climate change: results from six dynamic global vegetation
430 models. *Global Change Biology* *7*, 357-373. doi:10.1046/j.13652486.2001.00383.x
431
- 432 Dontsova, K., Balogh-Brunstad, Z. & Chorover, J. (2020). Plants as Drivers of Rock Weathering.
433 In *Biogeochemical Cycles* (eds K. Dontsova, Z. Balogh-Brunstad and G. Le Roux).
434 doi:10.1002/9781119413332.ch2
435
- 436 Drever, J. I. (1994). The effect of land plants on weathering rates of silicate minerals.
437 *Geochimica et Cosmochimica Acta* *58*, 2325-2332. doi: 10.1016/0016-7037(94)90013-2
438
- 439 Drewniak, B. A. (2019). Simulating Dynamic Roots in the Energy Exascale Earth System Land
440 Model. *Journal of Advances in Modeling Earth Systems*, *11*(1), 338–359. doi:
441 10.1029/2018MS001334
442
- 443 DuPont, S. T., Culman, S. W., Ferris, H., Buckley, D. H., & Glover, J. D. (2010). No-tillage
444 conversion of harvested perennial grassland to annual cropland reduces root biomass,
445 decreases active carbon stocks, and impacts soil biota. *Agriculture, ecosystems &*
446 *environment* *137*, 25-32. doi: 10.1016/j.agee.2009.12.021

- 447
448 Ebelmen, J. J. (1845). Sur les produits de la décomposition des espèces minérales de la famille
449 des silicates. *Annales des Mines* 12, 627-654.
450
- 451 Edgeworth, M., Richter, D. D., Waters, C., Haff, P., Neal, C. & Price, S. J. (2015). Diachronous
452 beginnings of the Anthropocene: The lower bounding surface of anthropogenic deposits.
453 *The Anthropocene Review*, 2, 33-58. doi: 10.1177/2053019614565394
- 454 Ellis, E.C., Goldewijk, K. K. , Siebert, S., Lightman, D. & Ramankutty, N. (2010).
455 Anthropogenic transformation of the biomes, 1700 to 2000. *Global Ecology and*
456 *Biogeography*, 19, 589-606. doi: 10.1111/j.1466-8238.2010.00540.x
- 457 Fan, Y., Miguez-Macho G., Jobbágy, E. G., Jackson, R. B. & Otero-Casal, C. (2017).
458 Hydrologic regulation of plant rooting depth. *Proceedings of the National. Academy of*
459 *Science USA*, 114, 10572-10577. doi: 10.1073/pnas.1712381114
- 460 Fisher, R. A., & Koven, C. D. (2020). Perspectives on the Future of Land Surface Models and
461 the Challenges of Representing Complex Terrestrial Systems. *Journal of Advances in*
462 *Modeling Earth Systems*, 12(4), 1–24. doi: [10.1029/2018MS001453](https://doi.org/10.1029/2018MS001453)
463
- 464 Fisher, R. A., Koven, C. D., Anderegg, W. R. L., Christoffersen, B. O., Dietze, M. C., Farrior, C.
465 E., Holm, J. A., Hurtt, G. C., Knox, R. G., Lawrence, P. J., Lichstein, J. W., Longo, M.,
466 Matheny, A. M., Medvigy, D., Muller-Landau, H. C., Powell, T. L., Serbin, S. P., Sato,
467 H., Shuman, J. K., ... Moorcroft, P. R. (2017). Vegetation demographics in Earth System
468 Models: A review of progress and priorities. *Global Change Biology*, 24(1), 35–54. doi:
469 10.1111/gcb.13910
470
- 471 Gupta, A.K. (2004). Origin of agriculture and domestication of plants and animals linked to
472 early Holocene climate amelioration. *Current Science* 87, 54-59.
- 473 Harsch, M.A. et al. (2009). Are treelines advancing? A global meta-analysis of treeline response
474 to climate warming. *Ecology Letters*, 12, 1040-1049. doi: 10.1111/j.1461-
475 0248.2009.01355.x
- 476 Hasenmueller, E.A., Gu, X., Weitzman, J. N., Adams, T. S., Stinchcomb, G. E., Eissenstat, D.
477 M., Drohan, P. J., Brantley, S. L., Kaye, J. P. (2017). Weathering of rock to regolith: The
478 activity of deep roots in bedrock fractures. *Geoderma*, 300, 11-31.
479 doi: 10.1016/j.geoderma.2017.03.020
- 480 Hauser, E., Richter, D. D., Markewitz, D., Brecheisen, Z., & Billings, S. A. (2020). Persistent
481 anthropogenic legacies structure depth dependence of regenerating rooting systems and
482 their functions. *Biogeochemistry* 147, 259-275. doi: 10.1007/s10533-020-00641-2
- 483 Haxeltine, A., & Prentice, I. C. (1996). BIOME3: An equilibrium terrestrial biosphere model
484 based on ecophysiological constraints, resource availability, and competition among plant
485 functional types. *Global Biogeochemical Cycles* 10, 693-709. doi: 10.1029/96GB02344
- 486 Hertel, D., Harteveld, M. A., & Leuschner, C. (2009). Conversion of a tropical forest into
487 agroforest alters the fine root-related carbon flux to the soil. *Soil Biology and*
488 *Biochemistry* 41, 481-490. doi: 10.1016/j.soilbio.2008.11.020
- 489 Hijmans, R. J., van Etten, J., Sumner, M., Cheng, J., Baston, D., Bevan, A., et al. (2019).

- 490 “Geographic Data Analysis and Modeling,” (CRAN, v. 3.0-7, 2019; [https://cran.r-](https://cran.r-project.org/web/packages/raster/raster.pdf)
491 [project.org/web/packages/raster/raster.pdf](https://cran.r-project.org/web/packages/raster/raster.pdf)).
- 492 Hurtt, G. C., Chini, L. P., Frolking, S., Betts, R. A., Feddema, J., Fischer, G., ... & Jones, C. D.
493 (2011). Harmonization of land-use scenarios for the period 1500–2100: 600 years of
494 global gridded annual land-use transitions, wood harvest, and resulting secondary lands.
495 *Climatic Change* 109, 117. doi: 10.1007/s10584-011-0153-2
- 496 Iversen, C.M. (2010). Digging deeper: Fine-root responses to rising atmospheric CO₂
497 concentration in forested ecosystems. *New Phytologist*, 186, 346-357.
498 doi: 10.1111/j.1469-8137.2009.03122.x
- 499 Jackson, R.B., Canadell, J., Ehleringer, J. R., Mooney, H. A., Sala, O.E. & Schulze, E. D. (1996).
500 A global analysis of root distributions for terrestrial biomes. *Oecologia*, 108, 389-411.
501 doi: 10.1007/BF00333714
- 502 Jaramillo, V. J., Ahedo-Hernández, R., & Kauffman, J. B. (2003). Root biomass and carbon in a
503 tropical evergreen forest of Mexico: changes with secondary succession and forest
504 conversion to pasture. *Journal of Tropical Ecology* 19, 457-464. doi: 10.
505 1017/S0266467403003493
- 506
- 507 Jobbagy, E. G. & Jackson, R. B. (2001) The distribution of soil nutrients with depth: Global
508 patterns and the imprint of plants. *Biogeochemistry*, 53, 51-77.
509 doi: 10.1023/A:1010760720215
- 510
- 511 Jordan, T. Ashley G. M., Barton, M. D., Burges, S. J., Farley, K. A., Freeman, K. H., Jeanloz, R.,
512 Marshall, C. R., Orcutt, J.A., Richter, F.M. et al. (Eds.). (2001). *Basic research*
513 *opportunities in Earth Science*. Washington D.C.: National Academy Press.
- 514
- 515 Kennedy, D., Swenson, S., Oleson, K. W., Lawrence, D. M., Fisher, R., Lola da Costa, A. C., &
516 Gentine, P. (2019). Implementing Plant Hydraulics in the Community Land Model,
517 Version 5. *Journal of Advances in Modeling Earth Systems*, 11(2), 485–513. doi:
518 [10.1029/2018MS001500](https://doi.org/10.1029/2018MS001500)
- 519
- 520 Kleidon, A. (2003). Global datasets of rooting zone depth inferred from inverse methods.
521 *Journal of Climate* 17, 2741-2722. doi: 10.1175/1520-
522 0442(2004)017<2714:GDORZD>2.0.CO;2
- 523
- 524 Kleidon, A. & Heimann M. (1998). A method of determining rooting depth from a terrestrial
525 biosphere model and its impacts on the global water and carbon cycle. *Global Change*
526 *Biology* 4, 275-286. doi: 10.1046/j.1365-2486.1998.00152.x
- 527
- 528 Lawrence, D. M., Fisher, R. A., Koven, C. D., Oleson, K. W., Swenson, S. C., Bonan, G.,
529 Collier, N., Ghimire, B., Kampenhout, L., Kennedy, D., Kluzek, E., Lawrence, P. J., Li,
530 F., Li, H., Lombardozzi, D., Riley, W. J., Sacks, W. J., Shi, M., Vertenstein, M., ... Zeng,
531 X. (2019). The Community Land Model Version 5: Description of New Features,
532 Benchmarking, and Impact of Forcing Uncertainty. *Journal of Advances in Modeling*
533 *Earth Systems*, 11(12), 4245–4287. doi: 10.1029/2018MS001583
- 534

535

536 Lawrence, D. M., & Slater, A. G. (2005). A projection of severe near-surface permafrost
537 degradation during the 21st century. *Geophysical Research Letters* 32, L24401.
538 doi:10.1029/2005GL025080.

539 Maeght, J. L., Rewald, B. & Pierret, A. (2013). How to study deep roots and why it matters.
540 *Frontiers in Plant Science*, 4, 299. doi: 10.3389/fpls.2013.00299

541 Nepstad, D.C., Carvalho, C. R. d., Davidson, E. A., Jipp, P. H., Lefebvre, P. A., Negreiros, G.
542 H., da Silva, E. D., Stone, T. A., Trumbore, S. E. & Vieira, S. (1994). The role of deep
543 roots in the hydrological and carbon cycles of Amazonian forests. *Nature*, 372, 666-669.
544 doi: 10.1038/372666a0

545 Nippert, J.B. & Knapp, A.K. (2007). Linking water uptake with rooting patterns in grassland
546 species. *Oecologia*, 153, 261-272. doi: 10.1007/s00442-007-0745-8

547 Oh, N. H., Hofmockel, M., Lavine, M. L., & Richter, D. D. (2007). Did elevated atmospheric
548 CO₂ alter soil mineral weathering?: An analysis of 5-year soil water chemistry data at
549 Duke FACE study. *Global Change Biology* 13, 2626-2641. doi: 10.1111/j.1365-
550 2486.2007.01452.x

551 Pawlik, L. (2013). The role of trees in the geomorphic system of forested hillslopes—A review.
552 *Earth-Science Reviews* 126, 250-265. doi: 10.1016/j.earscirev.2013.08.007

553 Pierret, A., Maeght, J. L., Clement, C., Montoroi, J. P., Hartman, C., & Gonkhamdee, S. (2016).
554 Understanding deep roots and their functions in ecosystems: An advocacy for more
555 unconventional research. *Annals of Botany*, 118, 621-625.
556 <https://doi.org/10.1093/aob/mcw130>

557 Ramankutty, N. & Foley, J.A. (1999). Estimating historical changes in global land cover:
558 Croplands from 1700 to 1992. *Global Biogeochemical Cycles* 13, 997-1027.
559 [doi: 10.1029/1999GB900046](https://doi.org/10.1029/1999GB900046)

560

561 Rasse, D. P., Rumpel, C., & Dignac, M. F. (2005). Is soil carbon mostly root carbon?
562 Mechanisms for a specific stabilisation. *Plant and soil* 269, 341-356. doi:
563 10.1007/s11104-004-0907-y

564

565 Richter, D. D. & Markewitz, D. (1995). How deep is soil? *BioScience*, 45, 600-609. doi:
566 10.2307/1312764

567

568 RStudio Team. (2017). “RStudio: Integrated development for R,” (RStudio Inc, Boston,
569 <http://www.rstudio.com/>).

570

571 Schenk, J. H. (2007). The shallowest possible water extraction profile: A null model for global
572 root distributions. *Vadose Zone Journal*, 7, 1119-1124.
573 doi: 10.2136/vzj2007.0119

574 Smithwick, E. A., Lucash, M. S., McCormack, M. L., & Sivandran, G. (2014). Improving the
575 representation of roots in terrestrial models. *Ecological Modelling* 291, 193-204.
576 doi: 10.1016/j.ecolmodel.2014.07.023

- 577
578 Stevens, N., Lehmann, C. E. R., Murphy, B. P. & Durigan, G. (2017). Savanna woody
579 encroachment is widespread across three continents. *Global Change Biology*, 23, 235-
580 244. doi: 10.1111/gcb.13409
- 581
582 Swank, W. T. (1986). Biological control of solute losses from forest ecosystems (Vol. 85). John
583 Wiley & Sons, New York.
- 584 Tang, J. Y., Riley, W. J., Koven, C. D., & Subin, Z. M. (2013). CLM4-BeTR, a generic
585 biogeochemical transport and reaction module for CLM4: Model development,
586 evaluation, and application. *Geosci. Model Dev.*, 6(1), 127–140. doi: 10.5194/gmd-6-
587 127-2013
- 588 Tiedje, J. M., Sexstone, A. J., Parkin, T. B., & Revsbech, N. P. (1984). Anaerobic processes in
589 soil. *Plant and Soil* 76, 197-212. doi: 10.1007/BF02205580
- 590
591 Traoré, O., Groleau-Renaud, V., Plantureux, S., Tubeileh, A., & Boeuf-Tremblay, V. (2000).
592 Effect of root mucilage and modelled root exudates on soil structure. *European Journal*
593 *of Soil Science* 51, 575-581. doi: 10.1111/j.1365-2389.2000.00348.x
- 594
595 Wang, J. A., Sulla-Menashe, D., Woodcock, C. E., Sonnentag, O., Keeling, R. F., & Friedl, M.
596 A. (2020). Extensive land cover change across Arctic–Boreal Northwestern North
597 America from disturbance and climate forcing. *Global Change Biology* 26, 807-822. doi:
598 [10.1111/gcb.14804](https://doi.org/10.1111/gcb.14804)
- 599
600 Whitford, W. G., & Duval, B. D. (2019). *Ecology of desert systems*. Academic Press.
- 601
602 Wilkinson, B. H., & McElroy, B. J. (2007). The impact of humans on continental erosion and
603 sedimentation. *Geological Society of America Bulletin* 119, 140-156. doi:
604 10.1130/B25899.1
- 605
606 Zhang, T., Barry, R. G., Knowles, K., Heginbottom, J. A., & Brown, J. (2008). Statistics and
607 characteristics of permafrost and ground-ice distribution in the Northern Hemisphere.
608 *Polar Geography* 31, 47-68. doi: 10.1080/10889370802175895
- 609
610 Zhang, Y., Niu, J., Yu, X., & Zhu, W. (2015). Effects of fine root length density and root
611 biomass on soil preferential flow in forest ecosystems. *Forest Systems* 24, e012.
612 doi: [10.5424/fs/2015241-06048](https://doi.org/10.5424/fs/2015241-06048)
- 613
614 Zhao, M., Heinsch, F. A., Nemani, R. R., & Running, S. W. (2005). Improvements of the
615 MODIS terrestrial gross and net primary production global data set. *Remote sensing of*
616 *Environment* 95, 164-176. doi: 10.1016/j.rse.2004.12.011
- 617
618 Zheng, X. (2001). Global vegetation root distribution for land modeling. *American*
619 *Meteorological Society* 2, 525-530. doi: 10.1175/1525-7
620 541(2001)002<0525:GVRDFL>2.0.CO;2
- 621
622 Ziegler, S.E., Benner, R., Billings, S.A., Edwards, K.A., Philben, M., Zhu, X. & Laganière, J.

623
624
625

(2017). Climate warming can accelerate carbon fluxes without changing soil carbon stocks. *Frontiers in Earth Science* 5, 2. doi:10.3389/feart.2017.00002